

# Preparation of psychrometric charts for water vapour in Martian atmosphere

David C. Shallcross \*

*Department of Chemical and Biomolecular Engineering, The University of Melbourne, Melbourne, Vic. 3010, Australia*

Received 9 March 2004; received in revised form 15 November 2004

Available online 18 January 2005

## Abstract

Psychrometric charts for condensing water vapour in Martian atmosphere at four different pressures are presented. The charts are based upon semi-theoretical equations and make use of published physical property data and correlations. The behaviour of the vapour phase is characterised by the Virial Equation of State truncated at the third term. The solubility of gas in water is also considered. The charts are constructed with the dry bulb temperature and absolute humidity scales as the orthogonal axes. Curves of constant adiabatic saturation temperature, constant relative humidity, constant gas specific volume and constant enthalpy deviation are plotted on the charts.

© 2005 Elsevier Ltd. All rights reserved.

*Keywords:* Humidity; Mars; Martian atmosphere; Psychrometric charts; Psychrometry

## 1. Introduction

An understanding of the conditions under which water vapour may condense from Martian atmosphere will be an important requirement for the future development of Mars. Already engineers have commenced design studies for the construction of greenhouses on the surface of Mars. The studies are investigating the feasibility of growing plants in a gaseous mixture of water vapour and Martian atmosphere. The designers of these greenhouses and other facilities planned for Mars need the ability to predict the conditions and extent to which condensation of water vapour will occur. They also need to be able to predict the properties of gaseous mixture of water vapour and Martian atmosphere as the humidity

of the mixture changes. Even in this age of computer aided design and physical property databases, engineers still find it useful to have physical property data presented graphically. Psychrometric charts are a way in which physical property data may be presented diagrammatically for systems in which one component of a gaseous mixture may condense. While accurate charts are readily available for the conventional water–air system, only recently have charts been prepared for other important systems. Just as importantly, until recently few charts had been prepared for pressure other than atmospheric [1].

The author described the theory behind the construction of psychrometric charts [1–3]. In this paper this method will be applied to construct a series of psychrometric charts for water vapour in Martian atmosphere. These charts may then be used in the future design of installations which may have industrial and horticultural applications.

\* Fax: +61 3 83 44 41 53.

E-mail address: [dshal@unimelb.edu.au](mailto:dshal@unimelb.edu.au)

**Nomenclature**

$B$	second virial coefficient
$c$	correlation coefficient
$C$	third virial coefficient
$C_p$	ideal gas heat capacity
$f$	enhancement factor
$g_1, g_2$	functions defined in Eqs. (A.13) and (A.14)
$\hat{h}$	real gas specific enthalpy
$\hat{h}_{\text{dev}}$	enthalpy deviation
$\hat{h}_f$	condensed phase enthalpy
$\hat{h}'_0$	enthalpy correction
$k_H$	Henry's law constant
MW	molecular weight
$P_C$	critical pressure
$P_V$	vapour pressure
$P_T$	total pressure
$R$	Universal gas constant
$T$	absolute temperature
$T_{\text{ad}}$	adiabatic saturation temperature
$T_C$	critical temperature
$T_{\text{datum}}$	enthalpy datum temperature

$T_r$	reduced temperature
$\hat{V}_C$	critical volume
$\hat{V}_{Vc}$	liquid molar volume
$x$	mole fraction
$Z_C$	critical compressibility factor

*Greek symbols*

$\phi$	relative humidity
$\kappa$	isothermal compressibility
$\lambda$	latent heat of vaporization
$\omega$	acentric factor

*Subscripts*

G	non-condensing gas component, i.e., Martian atmosphere
m	mixture
S	saturation condition
V	condensing vapour component, i.e., water vapour
W	water vapour

**2. Gas phase behaviour and saturation**

Martian atmosphere is predominantly carbon dioxide with relatively small amounts of nitrogen, argon, oxygen and carbon monoxide. At even relatively low pressures the gas mixture of water vapour and Martian atmosphere will not behave ideally. From the many different methods by which the non-ideal behaviour of gas may be characterized, the Virial Equation of State is used. This method is chosen because it is relatively simple to apply and because considerable data is available for the required parameters for the system studied. The Virial Equation of State truncated at the third term is:

$$\frac{P_T \hat{V}}{RT} = 1 + \frac{B_m}{\hat{V}} + \frac{C_m}{\hat{V}^2} \quad (1)$$

where  $P_T$  is the total pressure,  $\hat{V}$  is the molar volume of the gas mixture,  $R$  is the gas constant,  $T$  is the absolute temperature, and  $B_m$  and  $C_m$  are the second and third virial coefficients of the gas, respectively.

In the development of the equations which follows we shall assume that there are only two components in our system. The vapour component that readily condenses will be denoted  $V$ , and the gas component will be denoted  $G$ .

If  $x_G$  is the mole fraction of the non-condensing component (in this case nitrogen) and  $x_V$  is the mole fraction

of the condensing component (i.e. the alcohol) then for a binary system it may be shown that:

$$B_m = x_G^2 B_{GG} + 2x_G x_V B_{GV} + x_V^2 B_{VV} \quad (2)$$

$$C_m = x_G^3 C_{GGG} + 3x_G^2 x_V C_{GGV} + 3x_G x_V^2 C_{GVV} + x_V^3 C_{VVV} \quad (3)$$

Here  $B_{ii}$  is the second virial coefficient of pure component  $i$ ,  $B_{GV}$  is the second virial interaction (or cross) coefficient for the binary system,  $C_{iii}$  is the third virial coefficient of pure component  $i$ , and,  $C_{GGV}$  and  $C_{GVV}$  are the third virial interaction parameters. The virial coefficients are all functions of temperature alone, and are either known or may be estimated for most binary systems.

A gas is saturated with a vapour when the partial pressure of the vapour is equal to its vapour pressure at the particular temperature. For an ideal system we could write an expression relating the mole fraction of the condensing vapour component at saturation,  $V$ , to its vapour pressure:

$$x_{Vs} = \frac{P_V}{P_T} \quad (4)$$

and

$$x_{Gs} = \frac{P_T - P_V}{P_T} \quad (5)$$

where  $x_{Vs}$  and  $x_{Gs}$  are the mole fractions of components  $V$  and  $G$  respectively at saturation, and  $P_V$  is the vapour

pressure of component  $V$ . However, since the system is not ideal Hyland and Wexler [4] proposed the use of an enhancement factor. Eq. (4) becomes,

$$x_{Vs} = \frac{fP_V}{P_T} \quad (6)$$

A similar expression may be written for the non-condensing gas component  $G$ :

$$x_{Gs} = \frac{P_T - fP_V}{P_T} \quad (7)$$

The enhancement factor accounts for the effects of the dissolved gases and pressure on the properties of the condensed phase, and the effect of intermolecular forces on the properties of the moisture itself. Typically the value for the enhance factor does not exceed 1.05 for any given system at pressures up to 100 kPa [1]. The enhancement factor may be written in terms of the virial coefficients and the other properties of the system [4]:

$$\begin{aligned} \ln f = & \left[ \frac{(1 + \kappa P_V)(P_T - P_V) - \frac{1}{2}\kappa(P_T^2 - P_V^2)}{RT} \right] \hat{V}_{Vc} \\ & + \ln(1 - k_H x_{Gs} P_T) \\ & - \frac{2x_{Gs}^3(2 - 3x_{Gs})P_T^2}{(RT)^2} B_{GG}B_{GV} + \frac{x_{Gs}^2 P_T}{RT} B_{GG} \\ & - \frac{2x_{Gs}^2 P_T}{RT} B_{GV} - \left[ \frac{P_T - P_V - x_{Gs}^2 P_T}{RT} \right] B_{GG} \\ & - \frac{x_{Gs}^2(1 - 3x_{Gs})(1 - x_{Gs})P_T^2}{(RT)^2} B_{GG}B_{VV} \\ & + \frac{6x_{Gs}^2(1 - x_{Gs})^2 P_T^2}{(RT)^2} B_{VV}B_{GV} \\ & - \frac{2x_{Gs}^2(1 - x_{Gs})(1 - 3x_{Gs})P_T^2}{(RT)^2} B_{GV}^2 \\ & - \left[ \frac{P_V^2 - (1 + 3x_{Gs})(1 - x_{Gs})^3 P_T^2}{2(RT)^2} \right] B_{VV}^2 \\ & - \frac{3x_{Gs}^4 P_T^2}{2(RT)^2} B_{GG}^2 + \frac{3x_{Gs}^2(1 + 2x_{Gs})P_T^2}{2(RT)^2} C_{GGV} \\ & - \frac{3x_{Gs}^2(1 - x_{Gs})P_T^2}{(RT)^2} C_{GVV} \\ & - \left[ \frac{(1 + 2x_{Gs})(1 - x_{Gs})^2 P_T^2 - P_V^2}{2(RT)^2} \right] C_{VVV} \\ & + \frac{x_{Gs}^3 P_T^2}{(RT)^2} C_{GGG}. \end{aligned} \quad (8)$$

Here  $\kappa$  is the iso-thermal compressibility of the condensing component (i.e. the hydrocarbon),  $\hat{V}_{Vc}$  is the molar volume of the condensed component  $V$  (either as a liquid or a solid), and  $k_H$  is the Henry's Law constant to account for the solubility of component  $G$  in the condensed phase. For a given temperature and total pressure,  $P_T$ , Eqs. (7) and (8) may be solved iteratively for

the enhancement factor,  $f$ , and the mole fraction of component  $G$  at saturation,  $x_{Gs}$ . In practice this is done by first setting  $f = 1$ .  $x_{Gs}$  is then calculated using Eq. (7) and then this value is used in Eq. (8) to calculate an estimate for the enhancement factor,  $f$ . The value for  $x_{Gs}$  is then re-calculated. The cycle is then repeated until the values for  $f$  and  $x_{Gs}$  no longer change significantly between successive calculations.

The absolute humidity at saturation,  $H_s$ , is the mass of the vapour component  $V$  per mass of component  $G$ . It may be expressed in terms of the mole fractions of the two components in the gas phase at saturation:

$$H_s = \frac{x_{Vs}}{x_{Gs}} \frac{MW_V}{MW_G} \quad (9)$$

where  $MW_i$  is the molecular weight of component  $i$ .

Refs. [1,2] show how a psychrometric chart for a system may be calculated using the Virial Equation and the enhancement factor to account for the non-idealities in the system. The psychrometric charts are constructed with temperature plotted on the  $x$ -axis and absolute humidity on the orthogonal  $y$ -axis. The saturation line that describes the boundary of the humidity chart is drawn by plotting the absolute humidity at saturation,  $H_s$ , as a function of temperature for a specified total pressure. Series of curves for constant relative humidity, constant specific volume and constant adiabatic saturation temperature may be generated by use of the equations presented.

The relative humidity,  $\phi$ , is defined as the ratio of the mole fraction of the vapour component,  $x_V$ , in a given sample of the two-component mixture to the mole fraction,  $x_{Vs}$ , in a sample of the mixture which is saturated with the vapour component at that temperature. Thus,

$$\phi = \frac{x_V}{x_{Vs}} \quad (10)$$

In order to construct the curves of constant relative humidity an expression is required which relates the absolute humidity to the relative humidity, temperature and total pressure. Shallcross [1] derives the equation:

$$H = \frac{H_s \phi (1 - fP_V/P_T)}{1 - \phi fP_V/P_T} \quad (11)$$

To construct the constant relative humidity curves, the system pressure,  $P_T$ , is first specified. Then for a given value of  $\phi$ , the variables  $f$ ,  $H_s$  and  $P_V$  are calculated for varying temperatures. These values are then used in Eq. (11) to calculate the absolute humidity as a function of temperature. When plotted this data yields the constant relative humidity curves.

The specific volume of a humid mixture,  $v$ , is defined as the volume of the mixture per unit mass of the dry gas:

$$v = \frac{\hat{V}}{x_G MW_G} \quad (12)$$

Applying this definition and using Eq. (1), Shallcross [1] shows how the curves of constant specific volume may be plotted for a given system pressure.

The wet bulb temperature is usually considered as the temperature measured by a cylindrical thermometer, the outside surface of which is kept wet with the liquid of the condensing component  $V$ , in this case water. As the moist gas passes the thermometer some of the water evaporates resulting in a cooling effect that causes the temperature of the wet bulb thermometer to drop. The drier the gas, the greater the wet bulb depression. As the wet bulb temperature is a function of not only the dry bulb temperature and absolute humidity, but also such factors as the gas velocity past the thermometer, the diameter of the thermometer and the extent of radiative heat transfer, it is not possible to predict the wet bulb temperatures with precision. Consequently we choose to plot instead curves of constant adiabatic saturation temperature. It should be noted however that for the air–water system the curves of constant adiabatic saturation temperature coincide with curves of constant wet bulb temperature. This is because for the air–water system the Lewis Number is equal to one.

For the conventional air–water system, ASHRAE [5] defines the adiabatic saturation temperature,  $T_{ad}$ , as the temperature at which water (liquid or solid), by evaporating into moist air at a given dry bulb temperature,  $T$ , and absolute humidity,  $H$ , can bring air to saturation adiabatically at the same temperature,  $T_{ad}$ , while the pressure  $P_T$ , is maintained constant. The adiabatic saturation temperature is also known as the thermodynamic wet bulb temperature.

For a given G–V system, it may be defined as the temperature at which component  $V$ , present as either a liquid or a solid, by evaporating into the moist gas mixture at a given dry bulb temperature,  $T$ , and absolute humidity,  $H$ , can bring that mixture to saturation adiabatically at the same temperature,  $T_{ad}$ , while the pressure,  $P_T$ , is maintained constant. The method used to plot the curves of constant adiabatic saturation temperature is described in detail elsewhere [1,2].

The calculation and representation of the specific enthalpy of the gas mixture requires special attention. The specific of the two-component gas mixture is calculated by summing the ideal gas state enthalpy and the residual enthalpy:

WATER–MARTIAN ATMOSPHERE SYSTEM

100.0 kPa pressure

Enthalpy datum : liquid water 0.00 °C, 0.611 kPa  
 dry Martian atmosphere 0.00 °C, 101.3 kPa

Martian atmosphere composition :

CO <sub>2</sub>	95.49 mol %
N <sub>2</sub>	2.70 mol %
Ar	1.60 mol %
O <sub>2</sub>	0.13 mol %
CO	0.08 mol %

To obtain true enthalpy add enthalpy deviation to enthalpy at saturation.

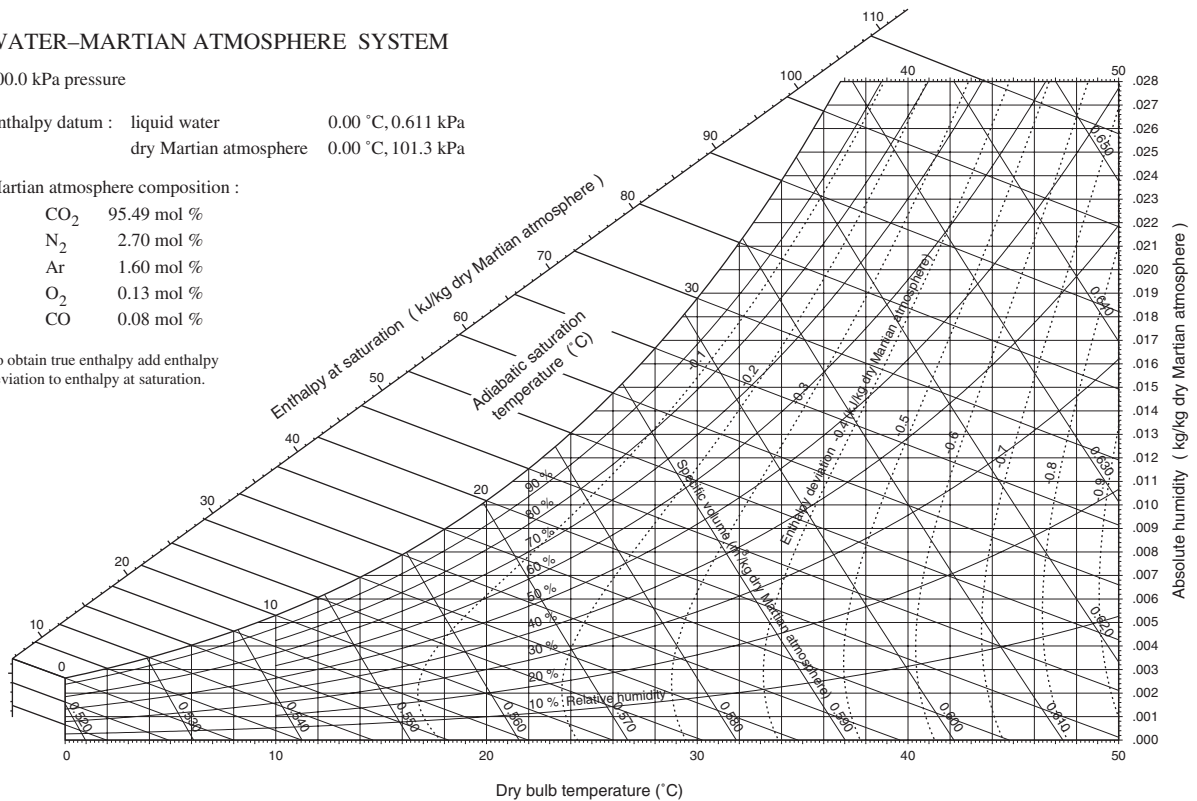


Fig. 1. Psychrometric chart for the water vapour in Martian atmosphere system at 100 kPa.

$$\begin{aligned} \hat{h} = & x_G \left( \hat{h}_{0G} + \int_{T_0}^T C_{P_G} dT \right) \\ & + x_V \left( \hat{h}_{0V} + \int_{T_0}^T C_{P_V} dT \right) \\ & + RT \left[ \left( T \frac{dB_m}{dT} - B_m \right) \frac{1}{\hat{V}_m} + \left( \frac{T}{2} \frac{dC_m}{dT} - C_m \right) \frac{1}{\hat{V}_m^2} \right] \end{aligned} \tag{13}$$

In this equation  $T_0$  is the enthalpy datum temperature,  $C_{PG}$  and  $C_{PV}$  are the ideal gas heat capacity of the gas and vapour respectively, and,  $\hat{h}_{0G}$  and  $\hat{h}_{0V}$  are the enthalpy corrections for both components necessary to ensure that the enthalpy,  $\hat{h}$ , is in fact zero at the enthalpy datum condition.

Because of the nature of the equations governing the construction of the constant adiabatic saturation temperature curves, lines of constant gas mixture enthalpy will lie nearly parallel to the adiabatic saturation temperature curves. Rather than plotting two sets of curves having nearly the same slope, which would result in a chart difficult to read, the gas mixture enthalpy data is presented in a different form. An enthalpy deviation term,  $\hat{h}_{dev}$ , is defined as being the difference between the true specific enthalpy of a gas mixture and the specific enthalpy of the gas saturated at its adiabatic saturation temperature:

$$\hat{h}_{dev} = \hat{h} - \hat{h}_{S,as} \tag{14}$$

When curves of constant enthalpy deviation are plotted on the psychrometric chart then the true specific enthalpy of a gas mixture can be determined by adding the enthalpy deviation for the point on the chart representing the mixture, to the enthalpy of the gas saturated at its adiabatic saturation temperature.

### 3. Chart preparation and production

Using the equations developed by the author [1,2] together with the relevant physical property data presented in Appendix A, psychrometric charts were prepared for the water vapour in Martian atmosphere at four different pressures.

A FORTRAN program was written incorporating the equations and physical property data for each system. This program generates output files of instructions in the Postscript graphics language. When sent to a suitable Postscript laser printer the psychrometric charts presented in Figs. 1–4 are produced. The charts are printed on a printer having a resolution of 600 dots per inch (23.6 dots per mm). This allows the curves on the charts to be plotted with extreme precision. On a

#### WATER–MARTIAN ATMOSPHERE SYSTEM

50.0 kPa pressure

Enthalpy datum : liquid water 0.00 °C, 0.611 kPa  
 dry Martian atmosphere 0.00 °C, 101.3 kPa

Martian atmosphere composition :

CO <sub>2</sub>	95.49 mol %
N <sub>2</sub>	2.70 mol %
Ar	1.60 mol %
O <sub>2</sub>	0.13 mol %
CO	0.08 mol %

To obtain true enthalpy add enthalpy deviation to enthalpy at saturation.

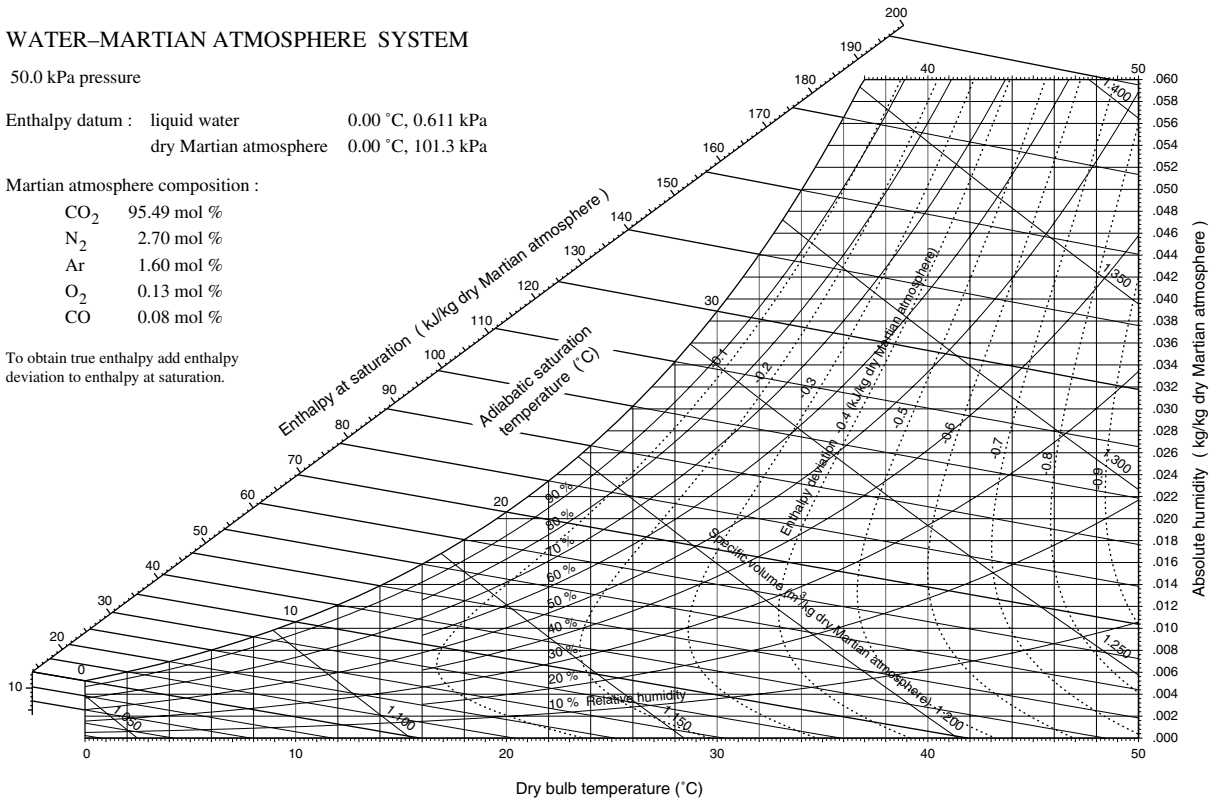


Fig. 2. Psychrometric chart for the water vapour in Martian atmosphere system at 50 kPa.

WATER–MARTIAN ATMOSPHERE SYSTEM

20.0 kPa pressure

Enthalpy datum : liquid water 0.00 °C, 0.611 kPa  
 dry Martian atmosphere 0.00 °C, 101.3 kPa

Martian atmosphere composition :

CO <sub>2</sub>	95.49 mol %
N <sub>2</sub>	2.70 mol %
Ar	1.60 mol %
O <sub>2</sub>	0.13 mol %
CO	0.08 mol %

To obtain true enthalpy add enthalpy deviation to enthalpy at saturation.

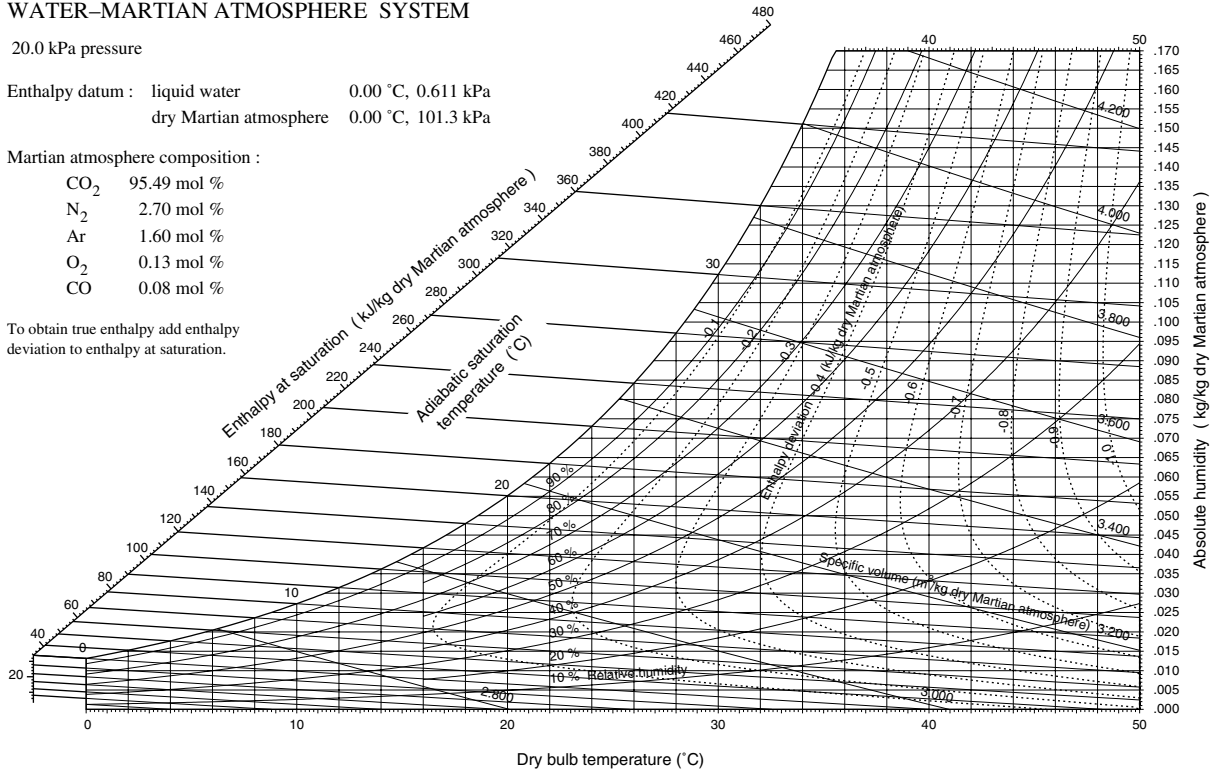


Fig. 3. Psychrometric chart for the water vapour in Martian atmosphere system at 20 kPa.

chart with a temperature range of 0–40 or 0–50 °C a plotting precision of 600 dots per inch is equivalent to placing a line with an accuracy of 0.01 °C.

The layout of Fig. 1 is typical of the psychrometric chart produced by the FORTRAN program. Dry bulb temperature is plotted on the *x*-axis with absolute humidity plotted on the *y*-axis. The relative humidity, specific volume, adiabatic saturation temperature and enthalpy deviation curves are all plotted as functions of dry bulb temperature and absolute humidity. The layout of the chart is self-explanatory. The enthalpy datum condition for the water is taken as liquid water at its vapour pressure at 0.01 °C.

The inclined scale for the enthalpy at saturation is slightly non-linear with units varying in size along the length of the scale. The scale is prepared by extrapolating the lines of constant adiabatic saturation temperature beyond the saturation curve to intersect the inclined scale. The values of enthalpy at saturation at each adiabatic saturation temperature then form the basis of the scale.

4. Discussion

The position of the saturation curve and hence the shape of the psychrometric chart is influenced by the

magnitude of the enhancement factor with temperature. Fig. 5 shows the variation in the enhancement factor with temperature for water vapour in Martian atmosphere at the four system pressures of 10 kPa, 20 kPa, 50 kPa and 100 kPa. In all cases the enhancement factor increases with increasing pressure and decreases with temperature. Also, for all systems, the enhancement factor falls in the range, 1.00 < *f* < 1.04.

As presented in Eq. (A.3), the enhancement factor is the sum of 15 terms. Analysis of the relative magnitudes of these terms show that just three terms dominate the sum, namely the fourth, fifth and sixth terms of the right-hand side of Eq. (8). Fig. 6 shows the values of these three terms in Eq. (8) for water vapour in Martian atmosphere at 100 kPa.

In the light of this analysis the expression for *ln f* in Eq. (8) may be approximated by the following equation without significant loss of accuracy:

$$\ln f = \frac{x_{G_s}^2 P_T}{RT} B_{GG} - \frac{2x_{G_s}^2 P_T}{RT} B_{GV} - \left[ \frac{P_T - P_V - x_{G_s}^2 P_T}{RT} \right] B_{GG} \quad (15)$$

Using this approximation for *f* results in an error of less than 0.1% compared to the value calculated using

WATER–MARTIAN ATMOSPHERE SYSTEM

10.0 kPa pressure

Enthalpy datum : liquid water 0.00 °C, 0.611 kPa  
dry Martian atmosphere 0.00 °C, 101.3 kPa

Martian atmosphere composition :

CO <sub>2</sub>	95.49 mol %
N <sub>2</sub>	2.70 mol %
Ar	1.60 mol %
O <sub>2</sub>	0.13 mol %
CO	0.08 mol %

To obtain true enthalpy add enthalpy deviation to enthalpy at saturation.

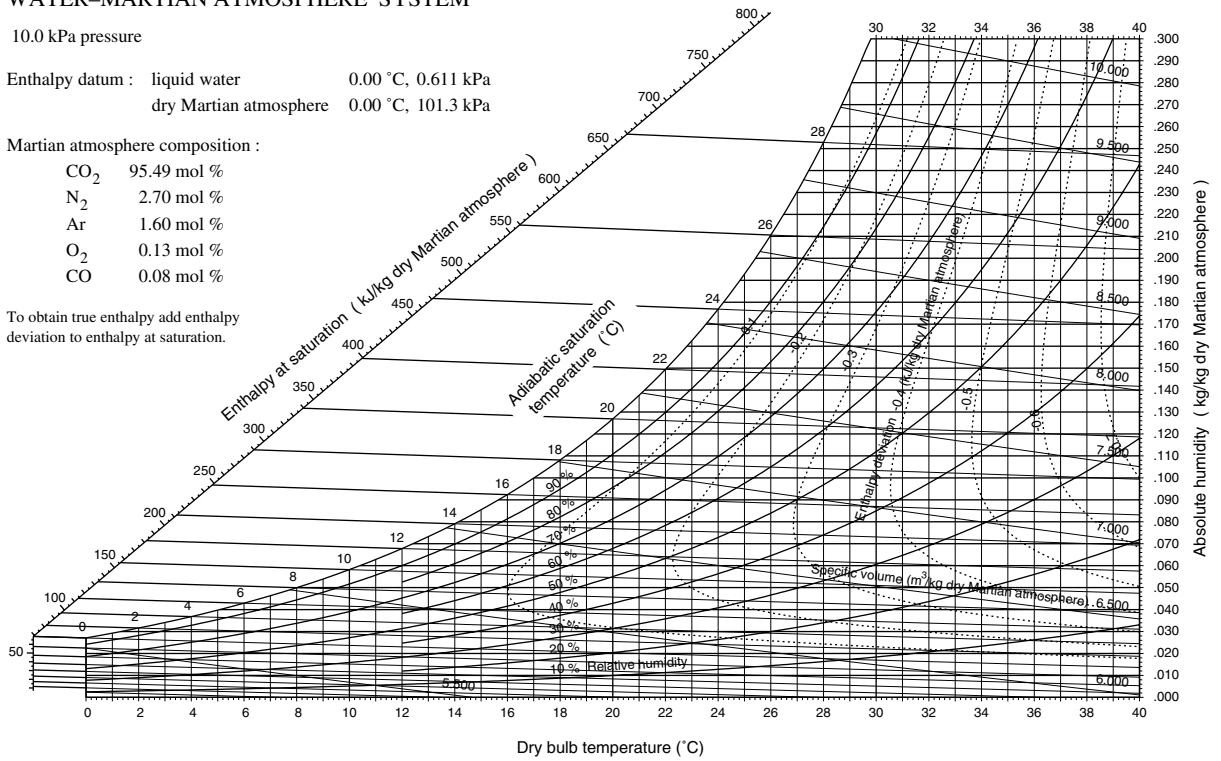


Fig. 4. Psychrometric chart for the water vapour in Martian atmosphere system at 10 kPa.

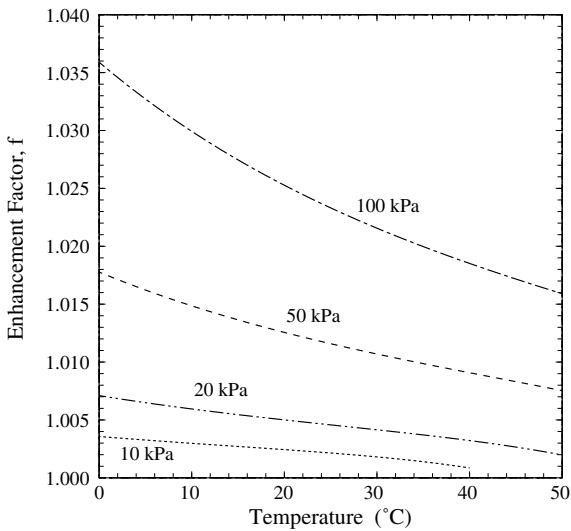


Fig. 5. Variation of enhancement with temperature and pressure for water vapour in Martian atmosphere.

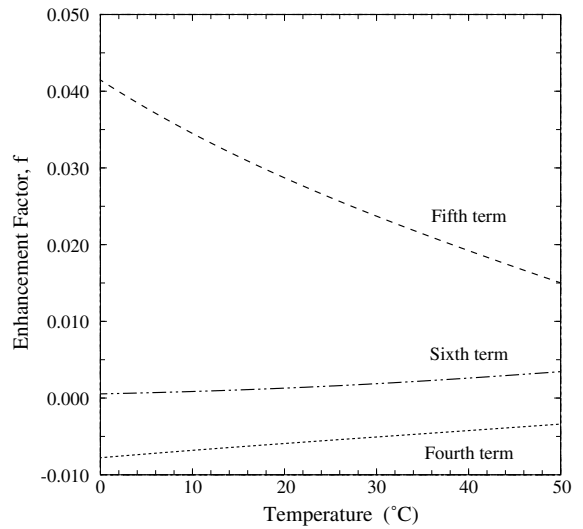


Fig. 6. Comparison of the three terms that dominate Eq. (8) for  $\ln f$ , for water vapour in Martian atmosphere at 100 kPa.

Eq. (8). Note that the four psychrometric charts presented in this paper were developed using Eq. (8) rather than Eq. (15) to calculate the enhancement factor,  $f$ .

In the above formulation neither the Henry's Law constant,  $k_H$ , the isothermal compressibility,  $\kappa$ , nor any of the third virial coefficients appear.

Whilst experimental data is not available to test the predictions made for charts prepared for water vapour in Martian atmosphere, the charts prepared for the water–air system using the same technique [2] agree extremely well with the widely accepted standard charts published by ASHRAE [5].

## 5. Concluding remarks

Using published physical property data and correlations, and equations developed earlier by the author, a series of high-precision psychrometric charts have been constructed for water vapour in Martian atmosphere. The fact that the model produces a chart in very close agreement to the widely accepted standard psychrometric chart for the water–air system supports the notion that the reliability of the charts produced are high.

## Appendix A. Physical property data

### A.1. Martian atmosphere composition

The National Aeronautics and Space Administration of the United States gives the composition of dry Martian atmosphere as 95.32 mol% CO<sub>2</sub>, 2.70 mol% N<sub>2</sub>, 1.60 mol% Ar, 0.13 mol% O<sub>2</sub> and 0.08 mol% CO with some other trace amounts [6]. As this composition does not sum to 100.00 mol%, in the present study the CO<sub>2</sub> content is adjusted so that the composition does sum to 100.00 mol%. The composition is assumed to be 95.49 mol% CO<sub>2</sub>, 2.70 mol% N<sub>2</sub>, 1.60 mol% Ar, 0.13 mol% O<sub>2</sub> and 0.08 mol% CO.

### A.2. Molecular weights, critical point and the acentric factor data

A number of the correlations used to estimate the required parameters call for information concerning the critical point and the acentric factor for each component. This information is presented in Table 1. As Martian atmosphere is a mixture, the data relating to its constitutive components is presented.

Table 1  
Molecular weight, critical point and the acentric factor data

Component	MW	$T_C$ (K)	$P_C$ (MPa)	$\hat{V}_C$ (m <sup>3</sup> /kmol)	$Z_C$	$\omega$
H <sub>2</sub> O	18.015	647.35	22.118	0.0635	0.261	0.348
CO <sub>2</sub>	44.010	304.20	7.3765	0.0940	0.274	0.225
N <sub>2</sub>	28.014	126.20	3.3944	0.0895	0.290	0.040
Ar	39.948	150.86	4.8737	0.0746	0.291	0.000
O <sub>2</sub>	31.999	154.58	5.0460	0.0736	0.288	0.021
CO	28.010	132.90	3.496	0.0931	0.295	0.049
Martian atmosphere	43.485	296.61	7.243	0.0923	0.271	0.216

Since some of the correlations that follow require single values of  $T_C$ ,  $P_C$ ,  $\hat{V}_C$ ,  $Z_C$  and  $\omega$  for air these must be calculated. Kay's rule is used to calculate a pseudo-critical temperature  $T'_C$  for air:

$$T'_C = \sum_i x_i T_{C_i} \quad (\text{A.1})$$

summed over all components.

For the pseudo-critical pressure,  $P'_C$ , the recommendations of Reid et al. [7] are followed:

$$P'_C = \frac{R(\sum_i x_i Z_{C_i}) T'_C}{(\sum_i x_i \hat{V}_{C_i})} \quad (\text{A.2})$$

The acentric factor for air is simply taken as

$$\omega' = \sum_i x_i \omega_i \quad (\text{A.3})$$

The pseudo-critical compressibility factor,  $Z'_C$ , is calculated from

$$Z'_C = Z^{(0)} + \omega' Z^{(1)} \quad (\text{A.4})$$

where  $Z^{(0)} = 0.2901$  and  $Z^{(1)} = -0.0879$  at the critical point [8].

The pseudo-critical volume,  $\hat{V}'_C$ , is calculated from

$$\hat{V}'_C = \frac{Z'_C R T'_C}{P'_C} \quad (\text{A.5})$$

Thus, for Martian atmosphere

$$T'_C = 296.61 \text{ K} \quad P'_C = 7.243 \text{ Mpa} \\ \hat{V}'_C = 0.09231 \text{ m}^3/\text{kmol} \quad Z'_C = 0.271 \quad \omega' = 0.216$$

### A.3. Second virial coefficients

Second virial coefficient data for a range of components may be related to temperature by a correlation of the form [9]:

$$B = \sum_{i=1}^4 c_i \left( \frac{298.15}{T} - 1 \right)^{i-1} \quad (\text{A.6})$$

where  $T$  is expressed in Kelvin, and  $B$  is expressed in cm<sup>3</sup>/mol. The values for the coefficients for the gaseous



Table 2  
Second virial coefficients for Eq. (A.6)

Component	$c_1$	$c_2$	$c_3$	$c_4$
CO <sub>2</sub>	-127	-288	-118	
N <sub>2</sub>	-4	-56	-12	
Ar	-16	-60	-10	
O <sub>2</sub>	-16	-62	-8	-3
CO	-9	-58	-18	

components of Martian atmosphere are tabulated in Table 2.

For water a modified version of the correlation is preferred [4]:

$$B = T(0.05820 - 0.012234e^{1734.29/T}) \quad (\text{A.7})$$

where  $B$  is expressed in cm<sup>3</sup>/mol and  $T$  is expressed in Kelvin.

#### A.4. Second virial cross-coefficients

The second virial cross-coefficients are estimated using the empirical correlation [10]:

$$B_{ij} = \hat{V}_{c_{ij}} \left[ c_1 + \omega_{ij}c_2 + \frac{c_3 + \omega_{ij}c_4}{T_{r_{ij}}} + \frac{c_5 + \omega_{ij}c_6}{T_{r_{ij}}^2} + \frac{c_7 + \omega_{ij}c_8}{T_{r_{ij}}^6} \right] \quad (\text{A.8})$$

where the critical properties  $T_{c_{ij}}$ ,  $\hat{V}_{c_{ij}}$  and  $\omega_{ij}$  are defined as:

$$T_{c_{ij}} = \sqrt{T_{c_i}T_{c_j}} \quad (\text{A.9})$$

$$\hat{V}_{c_{ij}} = \left( \frac{\hat{V}_{c_i}^{1/3} + \hat{V}_{c_j}^{1/3}}{2} \right)^3 \quad (\text{A.10})$$

$$\omega_{ij} = \frac{\omega_i + \omega_j}{2} \quad (\text{A.11})$$

In Eq. (A.8),

$$\begin{aligned} c_1 &= 0.442259 & c_2 &= 0.725650 \\ c_3 &= -0.980970 & c_4 &= 0.218714 \\ c_5 &= -0.611142 & c_6 &= -1.24976 \\ c_7 &= -0.11515624 & c_8 &= -0.189187 \end{aligned}$$

#### A.5. Third virial coefficients

The generalised empirical correlation is used to estimate the third virial coefficients [11]:

$$\frac{CP_C^2}{(RT)^2} = g_1 + \omega g_2 \quad (\text{A.12})$$

where  $C$  is the third virial coefficient,  $P_C$  is the critical pressure,  $T_C$  is the critical temperature,  $R$  is the Univer-

sal gas constant,  $\omega$  is the acentric factor, and  $g_1$  and  $g_2$  are both functions of the reduced temperature:

$$g_1 = 0.01407 + \frac{0.02432}{T_r^{2.8}} - \frac{0.00313}{T_r^{10.5}} \quad (\text{A.13})$$

$$g_2 = -0.02676 + \frac{0.01770}{T_r^{2.8}} + \frac{0.040}{T_r^{3.0}} - \frac{0.003}{T_r^{6.0}} - \frac{0.00228}{T_r^{10.5}} \quad (\text{A.14})$$

Hyland and Wexler [4] present a correlation for the third virial coefficient for water vapour for the pressure series form of the virial equation. Rewriting the correlation in terms of the volume series form, it becomes:

$$C_{\text{WWW}} = T^2 [752.82 - 2.31788e^{3645.09/T} + 1.49755e^{3468.58/T} - 14.2446e^{1734.29/T}] \times 10^{-4} \quad (\text{A.15})$$

where  $C_{\text{WWW}}$  is expressed in cm<sup>6</sup>/mol<sup>2</sup> and  $T$  is expressed in Kelvin.

#### A.6. Third virial cross-coefficients

The two third virial cross-coefficients for the each of the systems,  $B_{ijk}$  and  $B_{ijj}$ , are estimated using the empirical correlation of Orbey and Vera [11]. Brugge et al. [12] found this correlation to be good for estimating for cross-coefficients for three different systems. The correlation is

$$C_{ijk} = (C_{ij} C_{ik} C_{jk})^{1/3} \quad (\text{A.16})$$

where,

$$C_{ij} = \left( \frac{RT_{c_{ij}}}{P_{c_{ij}}} \right)^2 (g_1 + \omega_{ij}g_2) \quad (\text{A.17})$$

and  $g_1$  and  $g_2$  are both functions of  $T_{r_{ij}}$  defined in Eqs. (A.13) and (A.14). The cross-critical temperature and cross-acentric factor are defined as in Eqs. (A.9) and (A.11) respectively. The cross-critical pressure is defined as

$$P_{c_{ij}} = 4(Z_{c_i} + Z_{c_j})T_{c_{ij}} \left[ \left( \frac{Z_{c_i}Z_{c_j}}{P_{c_i}} \right)^{1/3} + \left( \frac{Z_{c_i}Z_{c_j}}{P_{c_j}} \right)^{1/3} \right]^3 \quad (\text{A.18})$$

#### A.7. Vapour pressure

Hyland and Wexler [4] present a correlation for the vapour pressure of water valid over the temperature range from 273.15 K to 473.15 K:

$$\ln P_V = \sum_{i=-1}^3 c_i T^i + 6.5459673 \ln T \quad (\text{A.19})$$

where  $P_V$  is the vapour pressure expressed in Pa,  $T$  is the absolute temperature in Kelvin, and,

$$c_{-1} = -5.8002206 \times 10^3 \quad c_2 = 4.1764768 \times 10^{-5}$$

$$c_0 = 1.3914993 \quad c_3 = -1.4452093 \times 10^{-7}$$

$$c_1 = -4.8640239 \times 10^{-2}$$

### A.8. Isothermal compressibility

A correlation for the isothermal compressibility of saturated liquid water over the range 0 to 150 °C is [13]

$$\kappa = \left( \frac{\sum_{i=0}^5 J_i t^i}{1 + J_6 t} \right) \times 10^{-11} \quad (\text{A.20})$$

where  $\kappa$  is expressed in  $\text{Pa}^{-1}$ ,  $t$  is expressed in °C and

for $0 \leq t \leq 100$ °C	for $100 \leq t \leq 150$ °C
$J_0 = 5.088496 \times 10$	$J_0 = 5.0884917 \times 10$
$J_1 = 6.163813 \times 10^{-1}$	$J_1 = 6.2590623 \times 10^{-1}$
$J_2 = 1.459187 \times 10^{-3}$	$J_2 = 1.3848668 \times 10^{-3}$
$J_3 = 2.008438 \times 10^{-5}$	$J_3 = 2.1603427 \times 10^{-5}$
$J_4 = -5.847727 \times 10^{-8}$	$J_4 = -7.2087667 \times 10^{-8}$
$J_5 = 4.104110 \times 10^{-10}$	$J_5 = 4.6545054 \times 10^{-10}$
$J_6 = 1.967348 \times 10^{-2}$	$J_6 = 1.9859983 \times 10^{-2}$

The isothermal compressibility of ice is given by Hyland and Wexler [4] as

$$\kappa = (8.875 + 0.0165T) \times 10^{-11} \quad (\text{A.21})$$

where  $\kappa$  is expressed in  $\text{Pa}^{-1}$ , and  $T$  is expressed in Kelvin.

### A.9. Molar volume of condensed phase

Hyland and Wexler [4] give a correlation for the density of water as a function of temperature. From this an expression may be written for the molar volume of water:

$$\hat{V}_{\text{Vc}} = \frac{-61692.295 + 291.8088T}{\sum_{i=0}^5 c_i T^i} \quad (\text{A.22})$$

where  $\hat{V}_{\text{Vc}}$  is the molar volume of water is expressed in  $\text{cm}^3/\text{mol}$ , and

$$c_0 = -2403.360201 \quad c_3 = -2.914492351 \times 10^{-4}$$

$$c_1 = -1.40758895 \quad c_4 = 3.73497936 \times 10^{-6}$$

$$c_2 = 0.1068287657 \quad c_5 = -2.1203787 \times 10^{-10}$$

Over the temperature range from 173.15 K to 273.15 K the molar volume of ice is [4]:

$$\hat{V}_{\text{Vc}} = 19.276404 - 4.50266 \times 10^{-4}T + 6.9468 \times 10^{-4}T^2 \quad (\text{A.23})$$

where  $\hat{V}_{\text{Vc}}$  is the molar volume of ice is expressed in  $\text{cm}^3/\text{mol}$ .

Table 3

Henry's Law coefficients for Eq. (A.24) for water vapour in various gases

Gas	$c_1$	$c_2$	$c_3$	Source
CO <sub>2</sub>	-7.25	0	0	Ref. [18]
N <sub>2</sub>	-181.587	8632.13	24.7981	Ref. [16]
Ar	-150.413	7476.27	20.1398	Ref. [14]
O <sub>2</sub>	-179.344	8747.55	24.4526	Ref. [15]

### A.10. Henry's law constants

The solubility of the gas component in the liquid is considered by making use of Henry's Law constants,  $k_{\text{H}}$ . Based upon the data and regressions presented in the volumes of the Solubility Data Series [14–18], Henry's Law constants may be related to temperature through equations of the form:

$$k_{\text{H}} = \frac{1}{\exp\left(c_1 + \frac{c_2}{T} + c_3 \ln(T)\right)} \quad (\text{A.24})$$

For the gases and liquids of interest values for  $c_1$ ,  $c_2$  and  $c_3$  are presented in Table 3.  $k_{\text{H}}$  is expressed in atm, and  $T$  is expressed in Kelvin.

For water in carbon monoxide, Cargill [17] recommends an extended form of the equation to predict the Henry's Law constant:

$$k_{\text{H}} = \frac{1}{\exp\left(-427.66 + \frac{15260}{T} + 67.843 \ln T - 0.07046T\right)} \quad (\text{A.25})$$

Henry's Law constant for a mixture may be calculated from the composition of the gas and the values of the Henry's Law constants for the individual components:

$$\frac{1}{k_{\text{H}}^{\text{MA-V}}} = \sum_j \frac{x_j}{k_{\text{H}}^{j-\text{V}}} \quad (\text{A.26})$$

where  $k_{\text{H}}^{\text{MA-V}}$  is the Henry's Law constant for the Martian atmosphere gas mixture in liquid V,  $x_j$  is the mole fraction of component  $j$  in the dry gas mixture and  $k_{\text{H}}^{j-\text{V}}$  is the Henry's Law constant for gas component  $j$  in liquid V.

Thus, Henry's law constant for air in liquid V is:

$$\frac{1}{k_{\text{H}}^{\text{MA-V}}} = \frac{0.9549}{k_{\text{H}}^{\text{CO}_2-\text{V}}} + \frac{0.0270}{k_{\text{H}}^{\text{N}_2-\text{V}}} + \frac{0.0160}{k_{\text{H}}^{\text{Ar}-\text{V}}} + \frac{0.0013}{k_{\text{H}}^{\text{O}_2-\text{V}}} + \frac{0.0008}{k_{\text{H}}^{\text{CO}-\text{V}}} \quad (\text{A.27})$$

### A.11. Heat capacity data

The ideal gas heat capacity for each component is assumed to be a cubic function of absolute temperature:

$$C_p = c_1 + c_2 T + c_3 T^2 + c_4 T^3 \quad (\text{A.28})$$

Reid et al. [7] tabulate the ideal gas heat capacity coefficients for a range of gases. These coefficients are presented in Table 4, after they have been converted so that  $C_P$  is expressed in J/g mol K and  $T$  is expressed in Kelvin.

$$\tilde{h}_f = \frac{-0.00115 + 4.21965t + 0.198652t^2 - 2.93514 \times 10^{-6}t^3 + 1.003624 \times 10^{-7}t^4}{1 + 0.0476516t} \quad (\text{A.30})$$

#### A.12. Enthalpy corrections

The enthalpy corrections,  $\tilde{h}'_{0G}$  and  $\tilde{h}'_{0V}$ , are applied in Eq. (13) to ensure that the enthalpy calculated is zero at the enthalpy datum condition. For Martian atmosphere,  $\tilde{h}'_{0G}$  is found from Eq. (13) by setting  $x_G = 1$  (and hence  $x_V = 0$ ),  $T = T_0 = 273.15$  K and  $P = 101.3$  kPa (the datum condition).

The datum condition for the water vapour is taken as liquid at the triple point (i.e.  $T = 273.16$  K and  $0.603$  kPa). In Eq. (13),  $x_V = 1$ ,  $T = T_0 = 273.16$  K and  $P = 0.603$  kPa.

The enthalpy corrections for the four components of interest are:

Martian atmosphere	60.38466 J/mol
water	7.43246 J/mol

#### A.13. Latent heat of vaporization

Keenan et al. [19] tabulate the latent heat of vaporization of water. Regression of the data between 0 and 100 °C yields the correlation:

$$\lambda = 2501.40 - 2.37341t + 0.000805207t^2 - 1.69018 \times 10^{-5}t^3 + 1.81383 \times 10^{-8}t^4 \quad (\text{A.29})$$

where  $\lambda$  is expressed in kJ/kg, and  $t$  is expressed in °C.

Table 4  
Ideal gas heat capacity coefficients for Eq. (A.28)

Gas	$c_1$	$c_2 \times 10^2$	$c_3 \times 10^5$	$c_4 \times 10^8$
CO <sub>2</sub>	19.80	7.344	-5.602	1.715
N <sub>2</sub>	31.15	-1.357	2.680	-1.168
Ar	20.80	$-3.211 \times 10^{-3}$	$-5.167 \times 10^{-3}$	0
O <sub>2</sub>	28.11	$-3.680 \times 10^{-4}$	1.746	-1.065
CO	30.87	-1.285	2.789	-1.272

#### A.14. Enthalpy of the condensed phase

McGowan [20] tabulates the enthalpy of water data to seven significant figures. Non-linear regression of the data between 0 and 100 °C yields the correlation:

where  $h_f$  is expressed in kJ/kg,  $t$  is expressed in °C, and, the enthalpy datum condition is taken as liquid at 0 °C.

#### References

- [1] D.C. Shallcross, Handbook of Psychrometric Charts, Chapman and Hall, London, 1997.
- [2] D.C. Shallcross, S.L. Low, Construction of psychrometric charts for systems other than water vapour in air, Chemical Engineering Research and Design 72 (1994) 763–776.
- [3] D.C. Shallcross, Psychrometric charts for hydrocarbon vapours in nitrogen, Calphad 20 (1996) 283–288.
- [4] R.W. Hyland, A. Wexler, Formulations for the thermodynamic properties of dry air from 173.15 K to 473.15 K, and of saturated moist air from 173.15 K to 372.15 K at pressure to 5 MPa, ASHRAE Transactions 89 (1983) 520–535.
- [5] ASHRAE, ASHRAE Handbook—Fundamentals SI Edition, American Society of Heating, Refrigerating and Air-Conditioning Engineers, Atlanta, USA, 1989.
- [6] NASA, Mars fact sheet. Available from: <<http://nssdc.gsfc.nasa.gov/planetary/factsheet/marsfact.html>> accessed 1 November, 2004.
- [7] R.C. Reid, J.M. Prausnitz, T.K. Sherwood, The Properties of Gases and Liquids, third ed., McGraw-Hill Book Company, New York, 1977.
- [8] B.I. Lee, M.G. Kesler, A generalised thermodynamic correlation based on the three-parameter corresponding states, AIChE Journal 21 (1975) 510–527.
- [9] H.V. Kehianian, Virial coefficients of selected gases, In: D.R. Lide (Ed.), CRC Handbook of Chemistry and Physics, 78th ed., CRC Press, Boca Racon, Florida, 1997, pp. 6-27–6-46.
- [10] K.S. Pitzer, Second virial coefficients for mixed gases of low polarity, Fluid Phase Equilibria 59 (1990) 109–113.
- [11] H. Orbey, J.H. Vera, Correlation for the third virial coefficient using  $T_c$ ,  $P_c$  and  $\omega$  as parameters, AIChE Journal 29 (1983) 107–113.
- [12] H.B. Brugge, L. Yurttas, J.C. Holste, K.R. Hall, Comparison of methods for calculating third virial coefficients: application to binary mixtures of CO<sub>2</sub> with N<sub>2</sub>, CH<sub>4</sub> and C<sub>2</sub>H<sub>6</sub>, Fluid Phase Equilibria 51 (1989) 187–196.

- [13] G.S. Kell, Density, thermal expansivity, and compressibility of liquid water from 0° to 150 °C: correlations and tables for atmospheric pressure and saturation reviewed and expressed on 1968 temperature scale, *Journal of Chemical Engineering Data* 20 (1975) 97–105.
- [14] H.L. Clever, *Solubility Data Series—vol. 4—Argon*, Pergamon Press, Oxford, 1980.
- [15] R. Battino, *Solubility Data Series—vol. 7—Oxygen and Ozone*, Pergamon Press, Oxford, 1981.
- [16] R. Battino, *Solubility Data Series—vol. 10—Nitrogen and Air*, Pergamon Press, Oxford, 1982.
- [17] R.W. Cargill, *Solubility Data Series—vol. 43—Carbon Monoxide*, Pergamon Press, Oxford, 1990.
- [18] P.G.T. Fogg, *Solubility Data Series—vol. 50—Carbon Dioxide*, Pergamon Press, Oxford, 1992.
- [19] J.H. Keenan, R.G. Keyes, P.G. Hill, J.G., *Steam Tables Thermodynamic Properties of Water Including Vapor, Liquid, and Solid Phases*, John Wiley and Sons, New York, 1978.
- [20] J.C. McGowan, Isothermal compressibility of liquids, In: R.C. Weast, M.J. Astle (Eds.), *CRC Handbook of Chemistry and Physics*, 60th ed., CRC Press, Boca Racon, Florida, 1980, F-16–F-20.